

Thermodynamics of baryonic matter with strangeness within non-relativistic energy density functional models

Ad. R. Raduta,¹ F. Gulminelli,² and M. Oertel³

¹*IFIN-HH, Bucharest-Magurele, POB-MG6, Romania*

²*ENSICAEN, UMR6534, LPC, F-14050 Caen cédex, France*

³*LUTH, CNRS, Observatoire de Paris, Université Paris Diderot, 5 place Jules Janssen, 92195 Meudon, France*

(Dated: October 16, 2018)

We study the thermodynamical properties of compressed baryonic matter with strangeness within non-relativistic energy density functional models with a particular emphasis on possible phase transitions found earlier for a simple n, p, e, Λ -mixture. The aim of the paper is twofold: I) examining the phase structure of the complete system, including the full baryonic octet and II) testing the sensitivity of the results to the model parameters. We find that, associated to the onset of the different hyperonic families, up to three separate strangeness-driven phase transitions may occur. Consequently, a large fraction of the baryonic density domain is covered by phase coexistence with potential relevance for (proto)-neutron star evolution. It is shown that the presence of a phase transition is compatible both with the observational constraint on the maximal neutron star mass, and with the present experimental information on hypernuclei. In particular we show that two solar mass neutron stars are compatible with important hyperon content. Still, the parameter space is too large to give a definitive conclusion of the possible occurrence of a strangeness driven phase transition, and further constraints from multiple-hyperon nuclei and/or hyperon diffusion data are needed.

PACS numbers: 26.60.-c 21.65.Mn, 64.10.+h,

Keywords:

I. INTRODUCTION

In the effort of building more realistic equations of state (EoS) on which the understanding of astrophysical issues as the structure and evolution of neutron stars (NS) or core-collapsing supernovae (CCSN) relies, special attention is presently paid to the behavior of baryonic matter at densities above nuclear matter saturation density. The subject is challenging as experimental data are too scarce to satisfactorily constrain the respective interactions, in particular if non-nucleonic degrees of freedom are involved.

Though, simple energetic arguments show that no reliable description can be conceived without considering strangeness [1]. As such it is hoped that astrophysical observations can eventually supplement the missing knowledge so far attained in terrestrial laboratories. An example in this sense is the present debate about the measurement of very massive neutron stars, and the associated core composition. The early conclusions ruling out hyperons from the NS core seem to be refuted by recent relativistic and non-relativistic mean-field models showing that a sufficiently repulsive hyperon-nucleon (Y - N) and hyperon-hyperon (Y - Y) interaction at high densities is able to reconcile the two solar mass measurements corresponding to PSR J1614-2230 [2] and PSR J0348+0432 [3] with the onset of strangeness [4–8] without necessarily a very early deconfinement transition circumventing the hyperon puzzle [9]. The presence of hyperons in dense stellar matter is expected to have important astrophysical consequences. We can recall for instance the modification of the neutron star cooling rate due to hyperonic Urca processes [10, 11] leading to very fast cooling for stars with a mass high enough to allow for the onset of hyperons, a result, however, very sensitive to hyperonic pairing [12], and thus subject to large uncertainties. By allowing for weak

non-leptonic reactions ($N + N \leftrightarrow N + Y$, $N + Y \leftrightarrow Y + Y$), direct and modified hyperonic Urca and strong interactions ($Y + Y \leftrightarrow N + Y$, $Y + Y \leftrightarrow Y + Y$) hyperons are also shown to impact on bulk viscosity and, thus, damp r-mode instabilities [13].

Most of the predictions are done within mean-field models. However, because of generic attractive and repulsive couplings between the different baryonic species, phase transitions could, in principle, be faced. An example is the liquid-gas phase transition occurring in nuclear matter. If there is a phase transition the mean-field solutions should be replaced by the Gibbs construction in the phase coexisting domains, thus modifying the equation of state. The occurrence of a phase transition in strange compressed baryonic matter has already been discussed in Ref. [14], where a new family of neutron stars characterized by much smaller radii than usually considered was predicted. However, very attractive hyperon-hyperon couplings were considered in that study, which presently appear ruled out by the experimental information on the ground state energy of double-lambda hypernuclei.

A detailed study of the phase diagram of dense baryonic matter was recently undertaken in Ref. [15, 16] within a non-relativistic mean-field model based on phenomenological functionals. The models in Refs. [15, 16] considered a simplified setup, taking only (n, Λ) [15] and (n, p, Λ) [16] baryon mixtures into account. It was shown that under these assumptions first- and second- order phase transitions exist, and are expected to be explored under the strangeness equilibrium condition characteristic of stellar matter. Two astrophysically relevant consequences have been worked out. In Ref. [16] it has been demonstrated that in the vicinity of critical points the neutrino mean-free path is dramatically reduced, such that the neutrino transport can be considerably affected. Ref. [17] shows within a spherical simulation that, if during the proto-

neutron star contraction after bounce the phase coexistence region is reached, a mini-collapse is induced, leading to pronounced oscillations of the proto-neutron star.

Our previous work suffers nevertheless of two major limitations. First, we considered the strangeness degree of freedom as fully exhausted by the Λ hyperon. If the hyperonic couplings are such that Σ^- or Ξ^- are more abundant than Λ , as predicted by a series of models, the extension and localization of phase coexistence domains will be different. Moreover, the possible dominance of a charged hyperon would impact on the direction of the order parameter and change the stability of the phase diagram with respect to the electron gas. In the extreme case, it could even make it disappear for neutron star matter.

Secondly, the previous study [15, 16] employs only one specific model, a phenomenological energy density functional, with one parameter set, assuming in particular a strongly attractive hyperon-hyperon interaction. The most recent analysis [18, 19] of double- Λ hypernuclei now tend to suggest a very small attraction in the Λ - Λ channel, though experimental data are still very scarce and extrapolations to infinite matter uncertain. Moreover accurate fits exist of microscopic Brueckner calculations [20] providing functionals which are consistent with the available experimental data on nucleon- Λ phase shifts. This can give some guidance on the functional in the nucleon- Λ channel, although it is known that such models fail to reproduce the existence of very massive neutron stars.

The aim of the present paper is thus twofold. Firstly, to investigate the phase diagram of the whole baryonic octet. Secondly, to test the sensitivity of the strangeness-driven phase transition on the hyperonic coupling constants. Both NY and YY channels will be considered. Since most experimental constraints concern the Λ -hyperon, to avoid proliferation of uncontrolled parameters, we will consider for this study only the simplest mixture $(n, p, \Lambda) + e$ which accounts for the three relevant densities: baryonic, charge/leptonic and strangeness.

The paper is organized as follows. Section II briefly presents the model and the phenomenology of the phase transition. The phase diagram of purely baryonic, as well as charge-neutral baryonic matter with leptons are spotted in Sections IV and V. The model dependence of the results is analyzed in Section VI by considering alternative density functionals for the N - Y and Y - Y -interactions and various values for the coupling constants. Conclusions are drawn in Section VII.

II. THE MODEL

In non-relativistic mean-field models, the total energy density of homogeneous baryonic matter is given by the sum of mass and kinetic energy densities of different particle species and the potential energy density:

$$\begin{aligned} e_B(\{n_i\}) &= \sum_{i=n,p,\Lambda,\Sigma,\Xi} \left(n_i m_i c^2 + \frac{\hbar^2}{2m_i} \tau_i \right) + e_{pot}(\{n_i\}) \\ &= e_B(n_B, n_S, n_Q), \end{aligned} \quad (1)$$

where $n_B = \sum_i n_i B_i$; $n_S = \sum_i n_i S_i$; $n_Q = \sum_i n_i Q_i$ represent the baryon, strangeness and charge number densities, respectively, corresponding to the three good quantum numbers assuming equilibrium with respect to strong interaction. The particle and kinetic energy densities can be expressed in terms of Fermi-Dirac integrals,

$$n_i = \frac{1}{2\pi^2 \hbar^3} \left(\frac{2m_i}{\beta} \right)^{\frac{3}{2}} F_{\frac{1}{2}}(\beta \tilde{\mu}_i); \quad \tau_i = \frac{1}{2\pi^2 \hbar^5} \left(\frac{2m_i}{\beta} \right)^{\frac{5}{2}} F_{\frac{3}{2}}(\beta \tilde{\mu}_i), \quad (2)$$

with $F_\nu(\eta) = \int_0^\infty dx \frac{x^\nu}{1 + \exp(x - \eta)}$. $\beta = T^{-1}$, m_i and $\tilde{\mu}_i$ denote, respectively, the inverse temperature, the effective i -particle mass and the effective chemical potential of the i -species self-defined by the single-particle density. The effective chemical potentials are related to the chemical potentials

$$\mu_i = \frac{\partial e_B}{\partial n_i} \quad (3)$$

via

$$\tilde{\mu}_i = \mu_i - U_i - m_i c^2, \quad (4)$$

where $U_i = \left. \frac{\partial e_{pot}}{\partial n_i} \right|_{n_j, j \neq i}$ are the self-consistent mean field single-particle potentials.

The potential energy density should in principle account for all possible couplings between nucleonic and hyperonic species, N - N , N - Y and Y - Y . The nuclear structure data constrain satisfactorily the N - N -interaction up to densities close to the normal nuclear saturation density and moderate isospin asymmetries, such that well constrained and reliable expressions for this functional, including isospin dependent effective masses and currents are available. The situation is much less clear for higher densities, strong isospin asymmetries as well as for channels containing hyperons. The most general expression of these potential energies can be expanded in a polynomial form

$$e_{pot}(n_C, n_{C'}) = \sum_{k,m} a_{CC'}^{(k,m)} n_C^k n_{C'}^m \quad (5)$$

As a guideline to characterize the couplings, the single particle potentials of baryon C in pure C' -matter are employed: $U_C^{(C')}(n_{C'}) = \partial e_{pot}(n_C, n_{C'}) / \partial n_C |_{n_C=0}$. The coupling constants $a_{CC'}^{(k,m)}$ can then be adjusted to reproduce standard values of these potentials at some reference density, obtained within a (model dependent) analysis of the available experimental data.

A Skyrme-like expression has been frequently employed for the energy density, where the contribution of channel CC' to the potential energy density is given by

$$\begin{aligned} e_{CC'}(n_C, n_{C'}) &= a_{CC'} n_C n_{C'} + c_{CC'} n_C n_{C'} \left(n_C^{\gamma_{CC'}} + n_{C'}^{\gamma_{CC'}} \right); \\ & \quad a_{CC'} < 0; \quad c_{CC'} > 0 \quad \gamma_{CC'} > 0. \end{aligned} \quad (6)$$

This form, which depends on only three parameters for each channel, is the simplest expression which corresponds to a controlled compressibility and fulfills the

condition that $U_C^{(C')}(n_{C'})$ vanishes at vanishing C' -density $\lim_{n_{C'} \rightarrow 0} U_C^{(C')}(n_{C'}) \rightarrow 0$, and becomes highly repulsive at C' -high density $\lim_{n_{C'} \rightarrow \infty} U_C^{(C')}(n_{C'}) \rightarrow \infty$. Let us notice that this simple (and probably simplistic!) form together with the fact that we fix it at one given density implies a coupling between short- and long-range behaviors of $U_C^{(C')}$ and $U_C^{(C)}$ potentials, $U_C^{(C')}(n_{C'}) = a_{CC}n_{C'} + b_{CC}n_{C'}^{\gamma_{CC}+1}$, $U_C^{(C)}(n_C) = 2a_{CC}n_C + 2(\gamma_{CC} + 1)c_{CC}n_C^{\gamma_{CC}+1}$.

Concerning the channels including strangeness, the available experimental information is particularly scarce. Hypernuclei experiments only provide information on Λ^- , Σ^- and Ξ^- potential well depths in symmetric nuclear matter at saturation densities and, to a less accurate extent, on the Λ - Λ interaction potential. Based on a wealth of Λ -hypernuclear data produced in (π^+, K^+) reactions, the presently accepted value of $U_\Lambda^{(N)}(n_0)$ is considered to be ≈ -30 MeV [21]. $U_\Xi^{(N)}(n_0)$ is known to be attractive, too, ≈ -14 MeV, based on missing mass measurements in the (K^-, K^+) reaction on carbon [22]. The situation of $U_\Sigma^{(N)}(n_0)$ is ambiguous. On the one hand (π^-, K^+) reactions on medium-to-heavy nuclei point to a repulsive potential of the order of 100 MeV or less [23]. On the other hand, the observation of a ${}^4_2\text{He}$ bound state in a ${}^4\text{He}(K^-, \pi^-)$ reaction [24] pleads in favor of an attractive potential. Very few multi-hyperon exotic nuclei data exist so far and all of them correspond to double- Λ light nuclei. The Λ - Λ bond energy can be estimated from the binding energy difference between double- Λ and single- Λ hypernuclei,

$$\Delta B_{\Lambda\Lambda} = B_{\Lambda\Lambda}({}^A_{\Lambda\Lambda}Z) - 2B_\Lambda({}^A_{\Lambda}Z), \quad (7)$$

where

$$B_{\Lambda\Lambda}({}^A_{\Lambda\Lambda}Z) = B({}^A_{\Lambda\Lambda}Z) - B({}^A_{\Lambda}Z). \quad (8)$$

Measured bond energies are affected by huge error bars. Double-Lambda ${}^{10}_{\Lambda\Lambda}\text{Be}$ and ${}^{13}_{\Lambda\Lambda}\text{B}$ data suggest $\Delta B_{\Lambda\Lambda} \approx 5$ MeV [25] while ${}^6_{\Lambda\Lambda}\text{He}$ data point toward a lower value $\Delta B_{\Lambda\Lambda} = 0.67 \pm 0.17$ MeV [18, 19]. The bond energy can be interpreted as a rough estimation of the $U_\Lambda^{(\Lambda)}$ potential at the average Λ density $\langle n_\Lambda \rangle$ inside the hypernucleus [26]. The extrapolation of few body systems binding energies into mean-field quantities is, nevertheless, problematic. In this sense, the more attractive values extracted from larger nuclei could appear more appealing for the present application. Though, it is presently considered that the most accurate experimental data correspond to the Nagara event with a bond energy of 0.67 ± 0.17 MeV. In this work we shall therefore consider the latter value, $\Delta B_{\Lambda\Lambda} = 0.67$ MeV. In what regards the average Λ -density in light nuclei we shall use the value proposed in Ref. [26], $\langle n_\Lambda \rangle \approx n_0/5$.

It is clear that fixing the standard value of the potential at one specific density only constrains one parameter of the generic C - C' -interaction. This shows that any phenomenological mean-field parameterization is subject to large uncertainties.

In our previous studies [15, 16] we have employed the

Skyrme-based functional by Balberg and Gal [27],

$$e_{pot}^{(BG)}(\{n_i\}) = \sum_{i,j} e_{ij}^{(BG)}(n_i, n_j);$$

$$e_{ij}^{(BG)}(n_i, n_j) = \left(1 - \frac{\delta_{ij}}{2}\right) (a_{ij}n_i n_j + b_{ij}n_{i3}n_{j3} + c_{ij} \frac{n_i^{\gamma_{ij}+1}n_j + n_j^{\gamma_{ij}+1}n_i}{n_i + n_j}), \quad (9)$$

where n_i, n_j are the isoscalar densities for nucleons, and Λ -, Σ - and Ξ -hyperons. n_{i3} stands for the respective iso-vector densities and the values of $\gamma_{ij} =: \gamma$ are chosen identical for any (i, j) for simplicity. As one may notice, the same functional form is employed in all channels and the potential energy proposed by Eq. (9) deviates from the simple polynomial form of Eq. (6) truncated at low order because of the $1/(n_i + n_j)$ -dependence of the short-range term. The expressions of the single-particle potentials of baryon C in pure C - and, respectively, C' -matter are

$$U_C^{(C)}(n_C) = a_{CC}n_C + \frac{\gamma+1}{2}c_{CC}n_C^\gamma,$$

$$U_C^{(C')}(n_{C'}) = a_{CC}n_{C'} + c_{CC}n_{C'}^\gamma. \quad (10)$$

They show that fixing the potentials, introduces a correlation between the parameters governing repulsion and those governing attraction not present in the generic form of Eq. (5). As we will see, such a correlation is also present in BHF microscopically based energy functionals proposed in Ref. [20]. A deeper analysis with a larger number of models would, however, be necessary to check whether this particularity possibly affects the generality of our results. A study in this sense with relativistic models is in progress [28].

Ref. [27] proposes three sets of parameters corresponding to different stiffnesses $\gamma = 2, 5/3, 4/3$. For the sake of simplicity, a unique value is assumed for $a_{YY'}$ and $c_{YY'}$, $Y, Y' = \Lambda, \Sigma^-, \Sigma^0, \Sigma^+, \Xi^-, \Xi^0$. In Ref. [15, 16], the stiffest interaction proposed in Ref. [27], BGI, has been used. It is characterized by the values $\gamma = 2$, $a_{NN} = -784$ MeV fm³, $b_{NN} = 214.2$ MeV fm³, $c_{NN} = 1936$ MeV fm^{3\delta}, $a_{\Lambda N} = -340$ MeV fm³, $c_{\Lambda N} = 1087.5$ MeV fm^{3\gamma}, $a_{\Sigma N} = -340$ MeV fm³, $b_{\Sigma N} = 214.2$ MeV fm³, $c_{\Sigma N} = 1087.5$ MeV fm^{3\gamma}, $a_{\Xi N} = -291.5$ MeV fm³, $b_{\Xi N} = 0$, $c_{\Xi N} = 932.5$ MeV fm^{3\gamma}, $a_{YY} = -486.2$ MeV fm³, $b_{\Lambda Y} = 0$, $b_{\Xi Y} = 0$, $b_{\Sigma Y} = 428.4$ MeV fm³, $c_{YY} = 1553.6$ MeV fm^{3\gamma} and leads to the following values of the different interaction potential depths in symmetric matter at normal nuclear saturation density: $U_{\Lambda, \Sigma}^{(N)}(n_0) = -26.6$ MeV, $U_{\Xi}^{(N)}(n_0) = -22.8$ MeV, $U_Y^{(Y)}(n_0) = -19.4$ MeV, $U_Y^{(Y')}(n_0) = -38$ MeV. For the reference value $n_0/5$ BGI provides $U_Y^{(Y)}(n_0/5) = -12.8$ MeV, $U_Y^{(Y')}(n_0/5) = -13.6$ MeV, meaning that it is too attractive than present double hypernuclei data indicate.

We remind that out of parameter sets proposed in Ref. [27], BGI produces the highest neutron star maximum mass: the maximum mass exceeds $2M_\odot$ if only Λ 's are considered. However, if the full octet is accounted for, the maximum neutron star mass becomes too low, possibly due to a not sufficiently repulsive Y - Y interaction at high densities.

Though, as one may notice by comparison with experimental data, the $\Lambda\Lambda$, and, probably, ΣN interactions are too attractive at low densities. The same is true for the other two potentials proposed in Ref. [27], too. It is interesting to notice that BG-like parameterizations in agreement with hypernuclei experimental data and able to reach two solar mass neutron stars have been proposed in Ref. [4]. For the sake of easier comparison, to see how the phase diagram evaluated in [15, 16] evolves when the whole baryonic octet is accounted for, we will however stick to the original BGI in this paper.

To see to what extent the existence of a strangeness driven phase transition is conditioned by the poorly-constrained Y - Y -interaction, in section VI we will return to the simple case of a (N, Λ) -mixture. We will compare the Balberg and Gal parameterization with an energy density functional, where the N - N and Λ - N interactions have been fitted to a microscopic Brueckner-Hartree-Fock calculation (BSL) [20] and vary the parameters of the Λ - Λ interaction in both models. In particular we will show that qualitatively, in large regions of parameter space, the phase diagram does not depend on the exact parametrization employed.

III. THERMODYNAMIC ANALYSIS OF THE PHASE DIAGRAM

The phase diagram of a \mathcal{N} -component system is, at constant temperature, a \mathcal{N} -dimensional volume. The frontiers of the phase coexistence domain(s), $\{n_i^{\mathcal{P}_j}\}$; $i = 1, \dots, \mathcal{N}$; $j = 1, \dots, M$, are determined by the $(\mathcal{N} + 1)(M - 1)$ conditions of thermodynamic equilibrium between M different phases,

$$\begin{aligned} \left(\frac{\partial f}{\partial n_i}\right)_{\mathcal{P}_1} &= \dots = \left(\frac{\partial f}{\partial n_i}\right)_{\mathcal{P}_M} = \mu_i; \quad i = 1, \dots, \mathcal{N} \\ \left(-f + \sum_i n_i \frac{\partial f}{\partial n_i}\right)_{\mathcal{P}_1} &= \dots = \left(-f + \sum_i n_i \frac{\partial f}{\partial n_i}\right)_{\mathcal{P}_M} = P, \end{aligned} \quad (11)$$

where $f = e - Ts$, s and P stand for the free energy density, entropy density and, respectively, pressure. For a system to present a phase coexistence, its mean-field solutions should be more expensive in terms of free energy than the state mixing given by Eqs. (11). Mathematically, this is equivalent to the presence of a convexity anomaly of the thermodynamic potential in the density hyperspace. The number of coexisting phases is determined by the number of order parameters or, in terms of local properties, the number of spinodal instability directions. The last quantity is equal to the number of negative eigenvalues \mathcal{N}_{neg} of the free energy curvature matrix $C_{ij} = \partial^2 f / \partial n_i \partial n_j$, such that $M = \mathcal{N}_{neg} + 1$.

The problem of phase coexistence in a \mathcal{N} -component system can be reduced to a problem of phase coexistence in a one-component system by Legendre transforming the thermodynamical potential f with respect to the remaining $(\mathcal{N} - 1)$ -chemical potentials [29].

Under the condition of equilibrium with respect to the strong interaction, baryonic matter is a three-component sys-

tem with the densities (n_B, n_Q, n_S) as degrees of freedom. It is important to remark here that the use of S as a good quantum number does not imply that strangeness density n_S is conserved. In particular, along the strangeness equilibrium trajectory $\mu_S = 0$ considered in this study n_S obviously varies.

This reduces the dimensionality of the phase space from 8(=number of species) to 3. To further reduce the dimensionality for studying phase coexistence, one may then perform the Legendre transformation with respect to any set (μ_B, μ_S) , (μ_S, μ_Q) and (μ_B, μ_Q) . Formally the three choices should be considered in order to investigate all possible phase separation directions, as required by a complete study. Within the simpler (n, p, Λ) system studied in Ref. [16], which has the same dimensionality as the full octet, we found that the order parameter is always one dimensional. This means that a single Legendre transformation is enough to spot the thermodynamics provided that the order parameter is not orthogonal to the controlled density. The most convenient framework to easily access the physical trajectories is the one controlling the n_B -density:

$$\tilde{f}(n_B, \mu_S, \mu_Q) = f(n_B, n_S, n_Q) - \mu_S n_S - \mu_Q n_Q. \quad (12)$$

The coexisting phases, if any, will then be characterized by equal values of $\mu_B = \partial \tilde{f} / \partial n_B$ and P and the phase instability regions will be characterized by a back-bending behavior of $\mu_B(n_B)|_{\mu_S, \mu_Q}$.

IV. THE PHASE DIAGRAM OF THE (n, p, Y) -SYSTEM

Within this section we will analyze the phase diagram of pure baryonic matter with strangeness following the lines exposed in the previous section. We employ the Balberg and Gal energy density [27], parameterization BGI, see Section II. The upper panel of Fig. 1 illustrates the evolution of the baryonic chemical potential as a function of baryonic density at constant values of $\mu_S = 0$, $\mu_Q = 0$ and $T = 1$ MeV [38] while the bottom panel depicts the abundances of different nucleonic and hyperonic species. Three back-bending regions in $\mu_B(n_B)$ exist. We can see that each back-bending is strictly correlated with the onset of new species, and a decrease of abundances of species already present. Upon choosing $\mu_S = 0$, $\mu_Q = 0$, the hyperonic production thresholds are exclusively determined by the particle's rest mass and the interaction potentials. Since within the BGI parameterization, the Y - Y and Y - Y' interaction depends only very weakly on the particular channel, the rest mass effects dominate. The first strange particle to appear, at about $2.6n_0$ is therefore the less massive one, Λ . The three quasi-degenerate Σ -particles whose masses are 74 MeV higher than the Λ -mass, are produced starting from about $3.6n_0$. The most massive hyperons, the Ξ -particles, are the last to be created, at about $5.5n_0$. At high densities hyperons become more abundant than nucleons. This shows that having accurate Y - Y , Y - Y' , and N - Y interactions is as important as having reliable nucleonic ones.

Investigation of $P(\mu_B)$ and $\tilde{f}(n_B)$ (not shown) confirms that any back-bending can be cured by a Maxwell construction and that the linear combination of stable phases has a lower value

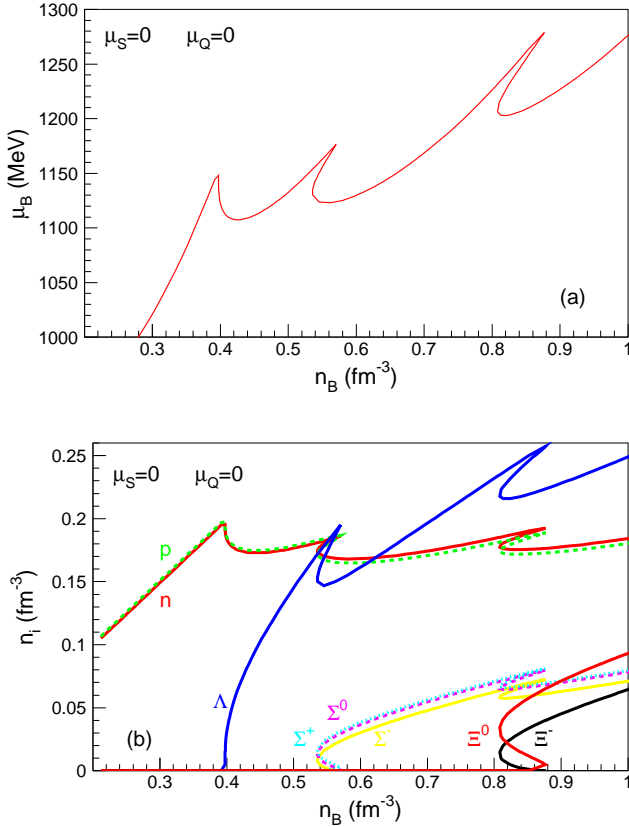


FIG. 1: (Color online) Baryonic chemical potential (top) and particle abundances (bottom) as a function of baryonic density for $\mu_S = 0$ and $\mu_Q = 0$ at $T = 1$ MeV, employing the BGI parameterization [27].

for \bar{f} than the mean-field solution, and corresponds thus to the energetically favored solution. This means that three distinct phase coexistence regions exist, induced by the onset of each hyperonic family.

Different thermodynamical conditions, i.e. different values of (μ_S, μ_Q) and T , will obviously change particle production thresholds, abundances, and the location of phase coexistence regions. By correspondingly changing the values of (μ_S, μ_Q) , the whole 3-dimensional phase diagram for a given temperature can be explored. Considering that in most astrophysically relevant situations the system is in equilibrium with respect to weak strangeness changing interactions, the most physically relevant part of the phase diagram is the cut corresponding to $\mu_S = 0$, which will be the only one considered within this work. The projections of the phase diagram of the (n, p, Y) mixture at the arbitrary temperature of 1 MeV to the $n_B - n_Q$ (panel (a)) and the $n_S - n_Q$ -plane (panel (b)) are represented in Fig. 2. The arrows indicate the directions of phase separation. Roughly speaking, two large phase coexistence domains exist: the first one corresponds to the appearance of Λ - and Σ -hyperons, while the second one is due to Cascades. They are well separated and extend over a significant total baryonic density range.

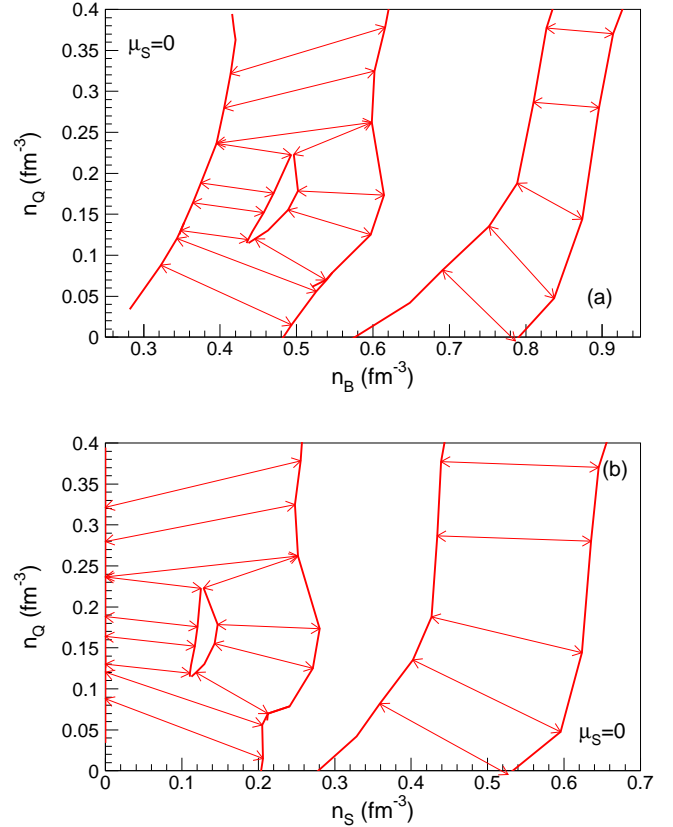


FIG. 2: (Color online) Phase diagram of the (n, p, Y) -system under strangeness equilibrium at $T = 1$ MeV as provided by the BGI parameterization [27] in the $n_B - n_Q$ (a) and $n_S - n_Q$ (b) planes. The arrows indicate the directions of phase separation.

At moderate values of μ_Q , where particle production is mainly dictated by the rest mass, the thresholds for Λ - and Σ -hyperons are pulled apart, and the phase coexistence regions corresponding to their respective onsets actually split up, as previously observed for $\mu_Q = 0$, see Fig. 1. At more important and negative μ_Q -values negatively charged particles are favored and consequently the Σ^- -threshold is shifted to lower densities and that for Σ^+ to higher ones. Upon increasing the absolute value of μ_Q finally the phase coexistence region triggered by the onset of Σ -hyperons merges with that for Λ -hyperons. The same happens for positive values of μ_Q , but with the roles of Σ^- and Σ^+ interchanged.

The direction of the order parameter is not constant over the phase coexistence region. The phase transition induced by Λ -hyperons is always characterized by a very small component of the order parameter along n_Q , as the transition is mainly triggered by neutral Λ -hyperons, as already emphasized in Ref. [16]. The Σ -induced phase transition has a small component along n_Q when the global Σ -charge is small, that is at low μ_Q -values, and a significant component at high μ_Q -values, i.e. for a high total Σ -charge. The Ξ -induced phase transition has an order parameter with important contribution

along n_Q whenever both Ξ^0 and Ξ^- are created as their total charge can not vanish. At high- μ_Q -values the Ξ^- production threshold is beyond the density domain considered for this study such that only Ξ^0 exist and consequently the charge dependence of the order parameter becomes very weak.

V. THE PHASE DIAGRAM OF (n, p, Y, e) -SYSTEM

The phenomenology of baryonic matter, as the one considered above, is purely academic. What is pertinent from the physical point of view is the phenomenology of electrically neutral matter, where the baryonic charge is compensated by leptonic charge. The net charge neutrality is a prerequisite condition for the thermodynamic limit to exist and corresponds to matter that constitutes compact objects where baryons exist together with leptons and photons. It is commonly accepted that the different sectors are in thermal and chemical equilibrium with respect to strong and electromagnetic interactions. Chemical equilibrium with respect to weak interactions can be satisfied or not depending on how fast the considered astrophysical system evolves compared with weak interaction rates. As such, β -equilibrium is reached in neutron stars while core-collapsing supernovae typically evolve out of β -equilibrium. To be as general as possible for the moment we shall not assume β -equilibrium. As mentioned before, we will, however, assume equilibrium with respect to strangeness changing weak interactions.

In the mean-field approximation, the total thermodynamic potential can be written as the sum of a baryonic, leptonic and photonic contribution, $f = f_B + f_L + f_\gamma$. Leptons and photons are well described by fermionic and, respectively, bosonic ideal gases [30]. The introduction of leptonic degrees of freedom does not increase the dimensionality of the problem [31] because the strict charge neutrality condition $n_Q = n_L$, imposed by thermodynamics, fixes n_Q in terms of leptonic density. Thus the charge degree of freedom is removed and the associated chemical potential, μ_Q becomes ill-defined. Within this work, $n_L = n_{e^-} - n_{e^+}$. The effect of other leptons, in particular muons, is considered beyond the scope of the present work and disregarded. Technically, the only modification with respect to the analysis in the case of pure baryonic matter discussed in the previous section is the replacement of the charge density with the (electron) leptonic one.

Adding an ideal gas contribution to the free energy might change the convexity, i.e. the stability of the system. Indeed, the thermodynamics of charge neutral matter can deeply differ from that of pure baryonic matter. As an example, the liquid-gas (LG) phase transition taking place in nuclear matter at sub-saturation densities is strongly quenched [31, 32] by the presence of electrons via the charge neutrality condition. This is due to the fact that a first order (LG) transition is associated with a macroscopic density fluctuation in direction of the order parameter. In the case of the nuclear LG transition, the order parameter has a strong component in charge direction, implying a macroscopic charge density fluctuation. This fluctuation is, however, strongly suppressed by the high incompressibility of the electron gas.

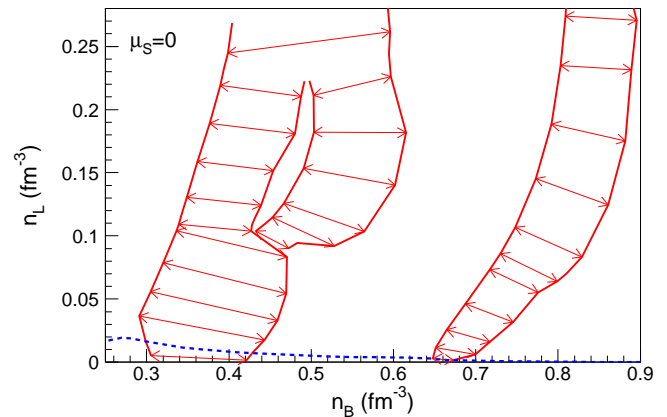


FIG. 3: (Color online) Phase diagram of the (n, p, Y, e) -system under strangeness equilibrium at $T=1$ MeV as provided by BGI parameterization [27] in the n_B - n_L -plane. The dotted curve marks the path corresponding to β -equilibrium.

Ref. [16] shows that, for the (n, p, Λ) system, the strangeness-driven phase transition is essentially not affected by the electrons. This is not surprising because Λ fluctuations are poorly correlated to the electric charge, see previous section, too. The situation is different here, because of the presence of charged hyperons. As discussed before, we can see in Fig. 2 that the order parameter has a significant component along the charge density especially for the Ξ -induced transition at low μ_Q -values, and it is in this domain that we expect the most dramatic alteration of the phase coexistence region.

The phase diagram of the (n, p, Y, e) -system under strangeness equilibrium at $T=1$ MeV is displayed in Fig. 3 in the plane n_B - n_L . As before, the arrows mark the directions of the order parameter. The pattern of the phase diagram is roughly the same as for pure baryonic matter: depending on μ_L , Λ - and Σ -hyperons are responsible for one or two phase transitions which extend over $0.3 \lesssim n_B \lesssim 0.6 \text{ fm}^{-3}$ and a Ξ -induced phase transition occurs at higher baryonic densities. The most important shrinking of the phase coexistence is obtained at low n_L -values. The direction of phase separation is rotated in the sense that its component along n_L gets smaller, which is expected since large electron density fluctuations are effectively suppressed.

VI. MODEL AND PARAMETER DEPENDENCE

The predictions of a phenomenological density-functional model depend dramatically on the functional form assumed for the energy density and the employed values of the coupling constants. As discussed in Section II, the functional form of the energy density in a non-relativistic phenomenological model is subject to large arbitrariness. The same is true for the coupling constants as the experimental data (a) correspond exclusively to low matter density, (b) are insufficient to constrain all the parameters of the potential energy

functional and (c) are often subject to large uncertainties, especially for the Y - Y (Y') channels. As a consequence, instead of one particular functional with one parameter set, one should rather consider different parameter sets and functional forms, satisfying the experimental conditions.

For this reason, we will first examine the correlation between the existence of the phase transition and the parameters of the Skyrme-based BG [27] energy density functional. To avoid proliferation of unconstrained parameters, the issue is considered in the simple case of a (n, p, Λ) mixture, which nevertheless satisfies the basic requirement of accounting for all relevant degrees of freedom, B , S , and Q . The two interaction channels which can be responsible of the phase transition are the N - Λ and the Λ - Λ one. Since the Y - Y interactions are poorly known, we first consider the extreme situation where the Λ - Λ coupling is completely absent.

A. The N - Y -interaction

The parameters of the N - Λ -channel, γ , $a_{N\Lambda}$ and $c_{N\Lambda}$, are considered as free variables which have to satisfy the unique condition $U_{\Lambda}^{(N)}(n_0) = -26.6$ MeV, keeping for simplicity the reference value of BGI. We consider $1.1 \leq \gamma \leq 3$, -1000 MeV $\text{fm}^3 \leq a_{N\Lambda} \leq -100$ MeV fm^3 and, in each case, calculate $c_{YN} = (U_{\Lambda}^{(N)}(n_0) - a_{N\Lambda} \cdot n_0) / n_0^{\gamma}$. The nuclear part remains the same as for BGI.

The upper panel of Fig. 4 plots, as a function of the stiffness parameter γ , the maximum values of the coupling constant $a_{N\Lambda}$ for which symmetric (N, Λ) -matter manifests phase coexistence along $\mu_S = 0$. As one may note, irrespective of γ , there is a wide range of values for the attractive Y - N coupling meaning that, in this model, phase coexistence in hyperonic matter is not conditioned by the Y - Y -interaction. The behavior of the Λ -potential in symmetric nuclear matter, $U_{\Lambda}^{(N)}(n_B) = \partial e_{pot}(n_N, n_{\Lambda}) / \partial n_{\Lambda} |_{n_{\Lambda}=0}$, as a function of nucleonic density is illustrated in panel (b) of Fig. 4 for few representative γ -values ($\gamma=1.72, 2$ and 3) and coupling constants situated at the extremities of the considered range ($a_{N\Lambda} = -900$ and -300 MeV fm^3), both inside and outside the domain compatible with phase coexistence, as indicated on the figure. We can see that a wide variety of density behaviors are compatible with the presence of a phase transition.

The new very precise astrophysical measurements of neutron star masses close to two solar masses [2, 3] represent a validity test for any astrophysical equation of state. As the rich recent literature testifies, this supplementary piece of information can neither confirm nor rule out the presence of hyperons in neutron stars. Indeed, while it is true that in principle any extra degree of freedom softens the EOS and, thus, lowers the maximum mass of the star, various models [4–8] prove that hyperons are compatible with the two solar mass constraint. The predictions of the β -equilibrium EOS at zero temperature for the neutron star mass as a function of central density obtained by solving the Tolman-Oppenheimer-Volkoff (TOV) [33] equations for hydrostatic equilibrium of a spheri-

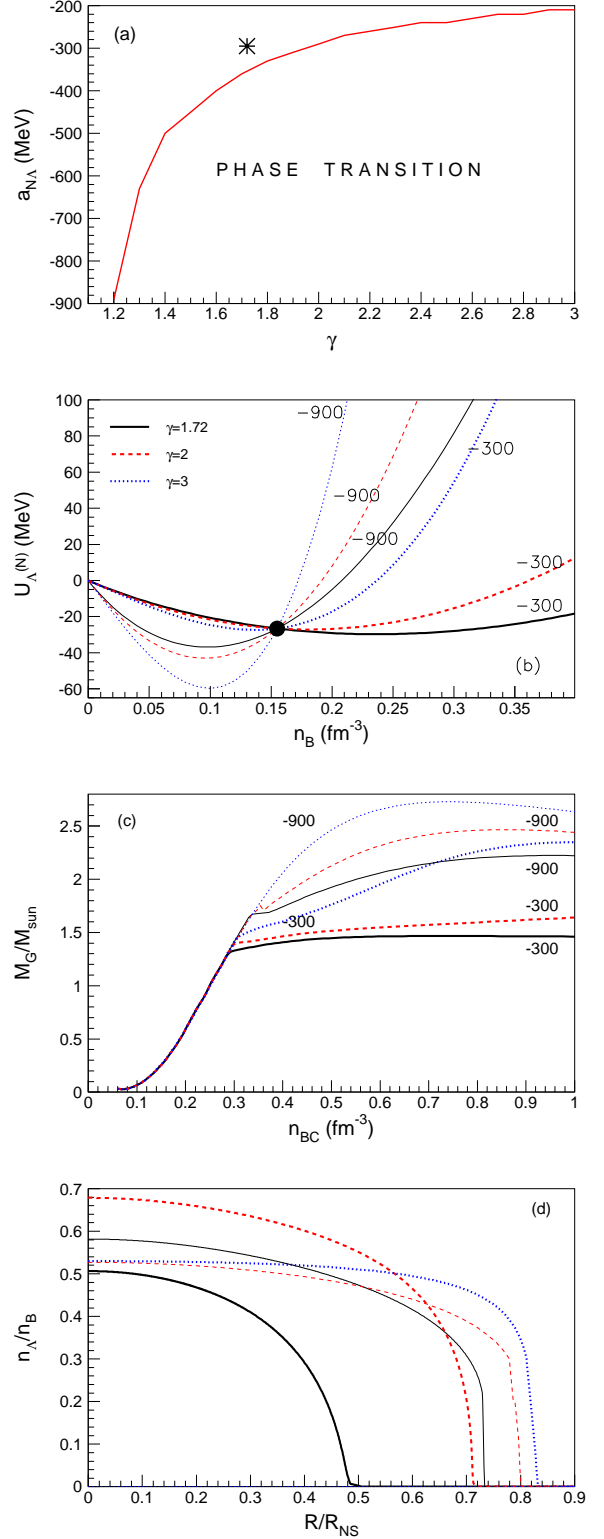


FIG. 4: (Color online) BG parameterization without Λ - Λ -interaction: (a) Limiting values of the coupling constant $a_{N\Lambda}$ for which, at different γ , the symmetric (N, Λ) -system at $T=0$ manifests strangeness driven phase transition along $\mu_S = 0$. The star marks the $(\gamma, a_{N\Lambda})$ values corresponding to the BSL NY -interaction (see text). (b) Nucleonic density dependence of the Λ potential in uniform symmetric nuclear matter $U_{\Lambda}^{(N)}(n_p + n_n)$ for different $(\gamma, a_{YN}[\text{MeV fm}^3])$ sets: (1.72, -900), (1.72, -300), (2, -900), (2, -300), (3, -900) and (3, -300). c_{YN} is determined such as $U_{\Lambda}^{(N)}(n_0) = -26.6$ MeV [27], see text; (c) Neutron star mass as a function of central baryon density for the (γ, a_{YN}) sets considered in (b); (d) Λ relative abundances as a function of normalized distance from the star center for the maximum

cal star,

$$\begin{aligned} \frac{dP(r)}{dr} &= -\frac{G}{r^2} \left[\varepsilon(r) + \frac{P(r)}{c^2} \right] \left[M(r) + 4\pi r^3 \frac{P(r)}{c^2} \right] \\ &\quad \cdot \left[1 - \frac{2GM(r)}{c^2 r} \right]^{-1}; \\ \frac{dM(r)}{dr} &= 4\pi \varepsilon(r) r^2 \end{aligned} \quad (13)$$

are represented in panel (c) of Fig. 4 for the parameter sets considered in panel (b).

Eq. (10) shows that, for the presently considered functional form of the energy density Eq.(9), a strong attraction at low density is associated with a strong repulsion at high density through the fixed $U_{\Lambda}^{(N)}(n_0)$. It is this peculiarity that makes possible to produce, by the most repulsive potentials, gravitational masses which largely exceed the reference $2M_{\odot}$ limit and have an important Λ -hyperon fraction. It is, however, important to stress that these results have to be considered as qualitative, because of the artificial absence of other hyperons than Λ 's. The inclusion of the full octet will obviously influence the mass-radius relationship quantitatively.

The bottom panel of Fig. 4 depicts, for the above considered NY interaction potentials and the maximum mass neutron star configuration, the Λ -relative abundances as a function of normalized distance from the star center. The reason why the curve corresponding to (3,-900) is missing is the extremely repulsive potential which prevent Λ s to appear. For the other interaction potentials one can see that hyperons not only exist, but they are abundant and populate most of the star's volume. The different central baryonic density values which correspond to the maximum mass configuration prevent a straightforward parallelism among the stiffness of the potential on one hand and the hyperonic relative density in the core and its extension on the other hand. This becomes obvious observing that the lowest and the highest fractions in the star core correspond to the softest considered potentials.

B. The Y - Y -interaction

We now turn to study the effect of the Λ - Λ interaction, both on the existence of the phase transition and on the maximum NS mass. To keep the same framework we shall consider the original BGI parameterization for the N - Λ channel, and the BG functional dependence in the Λ - Λ channel. Again, as in the case of the N - Λ interaction, we vary the Λ - Λ parameters keeping the Λ -potential in uniform Λ -matter at $1/5$ of nuclear saturation density fixed, $U_{\Lambda}^{(\Lambda)}(n_0/5)$, which leads to $c_{\Lambda\Lambda} = \left(U_{\Lambda}^{(\Lambda)}(n_0/5) - a_{\Lambda\Lambda} n_0/5 \right) \cdot 2/(\gamma+1)/(n_0/5)^{\gamma}$. The adopted value shall be $U_{\Lambda}^{(\Lambda)}(n_0/5) = -0.67$ MeV, see the discussion in Section II. We then consider different parameter sets $(\gamma, a_{N\Lambda}, a_{\Lambda\Lambda})$ in the ranges $1.2 \leq \gamma \leq 3$, -1000 MeV $\text{fm}^3 \leq a_{N\Lambda} \leq -200$ MeV fm^3 and -1000 MeV $\text{fm}^3 \leq a_{\Lambda\Lambda} \leq -100$ MeV fm^3 .

Adding the Λ - Λ long-range attractive - short-range repulsive interaction, the (n, p, Λ) toy system manifests phase co-

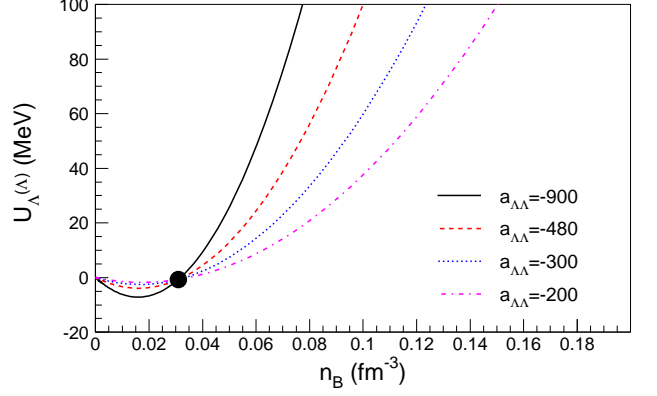


FIG. 5: (Color online) Λ -potential in uniform Λ -matter as a function of density corresponding to BGI parameterization with modified Λ - Λ interaction: $a_{\Lambda\Lambda} = -900, -480, -300$ and -200 MeV fm^3 and $\gamma = 2$.

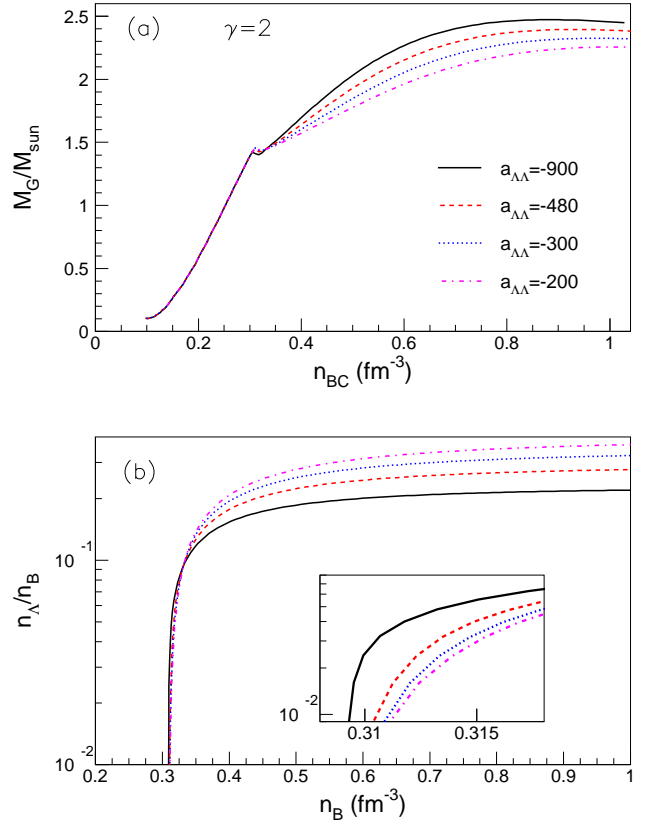


FIG. 6: (Color online) (a) Neutron star mass as a function of central density and (b) Relative Λ abundances as a function of baryonic density along the β -equilibrium path for the effective interaction potentials considered in Fig. 5.

existence in a much broader parameter range. More precisely, a strangeness-driven phase transition along the $\mu_S = 0$ path is obtained for almost all considered sets.

Fig. 5 illustrates $U_\Lambda^{(\Lambda)}(n_\Lambda = n_B)$ for $\gamma = 2$ and $a_{\Lambda\Lambda} = -900, -480, -300, -200$ MeV. As in the case of the N - Λ -channel, a strong attraction leads to a steep rise at high densities and a deep minimum localized at low densities, due to the fact that we fix the value at $n_0/5$ and the correlation between attraction and repulsion for the BG functional form.

Fig. 6 depicts the predictions of these potentials for the NS gravitational mass as function of central density (panel (a)) together with the Λ -relative abundances as a function of baryonic density along the beta-equilibrium trajectory (panel (b)). In all cases, for the N - Λ -channel the BGI parameter values have been employed. The relative ordering of the various curves is easily understandable for high central densities where the short range repulsion is effective: the stronger is the Λ - Λ repulsion, the smaller is the relative Λ density and the larger the obtained NS mass. Equally predictable is the fact that small differences in the low density attractive part of the potential result in minor modifications of the Λ -production threshold, to a large extent dictated by the N - Y interaction. Indeed, for the most attractive considered potential, Λ -hyperons emerge at a baryonic density only $3 \cdot 10^{-4} \text{ fm}^{-3}$ lower than that the one corresponding to the least attractive potential.

The calculations presented so far were all obtained with a phenomenological non-relativistic functional, that proposed by Balberg and Gal [27], both for the N - Λ and the Λ - Λ channel. One can therefore wonder if the observed phase transition is not a pathology of the assumed and largely arbitrary functional form of the energy density.

C. BHF N - Y interaction potentials

For more than fifteen years different microscopically motivated N - N and N - Y interaction potentials have been proposed. These functionals have all been adjusted to Brueckner-Hartree-Fock calculations hyper-nuclear matter based on different bare N - N and N - Y interactions, and are designed to perform calculations of hypernuclei [26, 34–36] and more recently hyper-nuclear matter [20, 37]. In all of these potentials, Y - Y interactions have been disregarded because of missing experimental constraints for the basic two-particle Y - Y interaction and the difficulties observed with BHF calculations including the insufficiently constrained bare Y - Y -interaction.

The two parametrizations designed for hyper-nuclear matter, Refs. [20, 37], rely on the same energy density functional,

$$e_{N\Lambda}^{(BSL)} = (a_\Lambda^0 + a_\Lambda^1 x + a_\Lambda^2 x^2) n_N n_\Lambda + (b_\Lambda^0 + b_\Lambda^1 x + b_\Lambda^2 x^2) n_N^{c_\Lambda} n_\Lambda + a_{\Lambda\Lambda}^{(BSL)} n_N^{c_{\Lambda\Lambda}} n_\Lambda^{d_{\Lambda\Lambda}+1}, \quad (14)$$

where $x = n_p/n_N$. They differ in the coupling constants values as the BHF calculations correspond to various treatments of the three-body forces and Y - N -potentials and predict significantly different Λ - and Σ^- -abundances [37]. For our applica-

tion we have chosen to use the Burgio-Schulze-Li parameterization [20] because of its stiffer $U_\Lambda^{(N)}(n_N)$ dependence.

Despite the functional dissimilarity between Eqs. (14) and (9), the two parameterizations can be bridged via the Λ -potential in uniform symmetric nuclear matter,

$$\begin{aligned} U_\Lambda^{(N)}(n_N) &= \frac{\partial e_{pot}^{(BSL)}(n_N, n_\Lambda)}{\partial n_\Lambda} \Big|_{n_\Lambda=0} \\ &= \frac{\partial e_{N\Lambda}^{(BSL)}(n_N, n_\Lambda)}{\partial n_\Lambda} \Big|_{n_\Lambda=0} \\ &= \left(a_\Lambda^0 + \frac{a_\Lambda^1}{2} + \frac{a_\Lambda^2}{4} \right) n_N + \left(b_\Lambda^0 + \frac{b_\Lambda^1}{2} + \frac{b_\Lambda^2}{4} \right) n_N^{c_\Lambda}. \end{aligned} \quad (15)$$

which, in both cases, is a polynomial in the baryonic density. Similarly to Eq. (10) a correlation between short- and long-range interactions is present in Eq. (15). We note that Eq. (15) can be mapped onto $\partial e_{pot}^{(BG)}/\partial n_\Lambda|_{n_\Lambda=0}$ provided that $\gamma = c_\Lambda = 1.72$, $a_{N\Lambda} = a_\Lambda^0 + a_\Lambda^1/2 + a_\Lambda^2/4 = -294.75 \text{ MeV fm}^3$, $c_{N\Lambda} = (b_\Lambda^0 + b_\Lambda^1/2 + b_\Lambda^2/4) = 462.75 \text{ MeV fm}^{3\gamma}$. The (1.72, -294.75) point is represented in Fig. 4 (a) by a star and sits outside the phase coexistence domain of a symmetric (N, Λ) mixture at strangeness equilibrium. We note that these values are very close to ($\gamma = 1.72$, $a_{\Lambda\Lambda} = -300 \text{ MeV fm}^3$) for which $U_\Lambda^{(N)}(n_N)$ is depicted in Fig. 4.

We have, however, to keep in mind that this functional gives an EoS which is much too soft and fails to reproduce $2M_\odot$ maximum neutron star mass [37]. This is shown in the bottom panel of Fig. 7, which depicts the NS mass as a function of central baryon number density. This is due to the lacking repulsion in the high density domain, meaning that probably the functional is not very reliable at the densities relevant for the phase transition. It is thus important at this point to stress that no firm conclusion can be drawn. It is certainly true that the phenomenological BG form is largely arbitrary; however the description of the nucleon-hyperon interaction in the BHF theory cannot be complete, neither.

As we have already stressed, the Y - Y interaction cannot be neglected in hyperonic matter. It could well be the source of missing repulsion in microscopic models. Due to the lack of information on this channel within microscopic calculations, for this channel we will adopt the simple polynomial form of BG, and supplement the BSL functional, Eq. (14), with it. The upper panel of Fig. 7 illustrates the maximum values of the coupling constant $a_{\Lambda\Lambda}$ for which phase coexistence occurs in symmetric $N\Lambda$ matter at various values of the stiffness parameter γ . The considered domains are $1.1 \leq \gamma \leq 3$ and $-1500 \leq a_{\Lambda\Lambda} \leq -100 \text{ MeV fm}^3$. As before, $c_{\Lambda\Lambda}$ is obtained from the condition $U_\Lambda^{(\Lambda)}(n_0/5) = -0.67 \text{ MeV}$. One can see that, in case of moderate N - Y -repulsion as it is the case for BSL, a phase coexistence can still be obtained, but it requires a considerable attraction in the Y - Y channel.

The effect of the Λ - Λ -interaction on the NS mass-central density relation and, respectively, the Λ -hyperon abundances in β equilibrium is represented in the bottom and middle panels of Fig. 7. The two considered Λ - Λ -interactions corre-

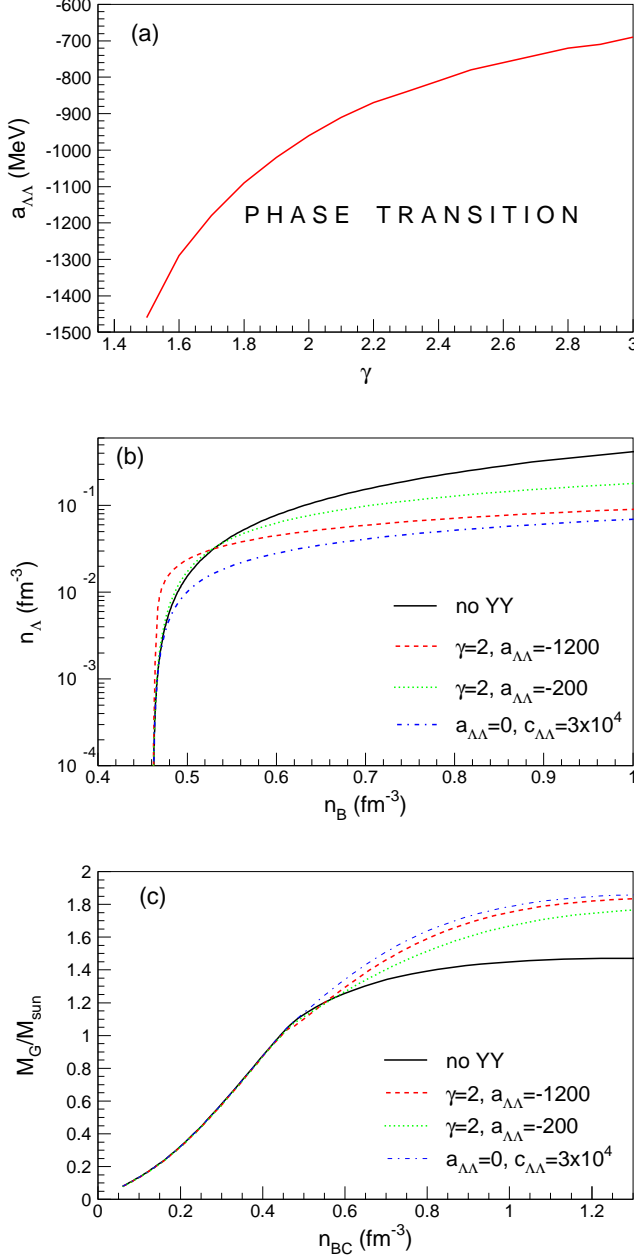


FIG. 7: (Color online) BSL parameterization + Λ - Λ -interaction: (a) Limiting values of the coupling constant $a_{\Lambda\Lambda}$ for which, at different γ , the symmetric (N, Λ) -system at $T=0$ manifests strangeness driven phase transition along $\mu_S = 0$; $c_{\Lambda\Lambda}$ is fixed via the condition $U_{\Lambda}^{(\Lambda)}(n_0/5) = -0.67 \text{ MeV}$; (b) Λ -density along the β -equilibrium path at $T=0$ for the original BSL potential and the cases in which BSL is supplemented with a Λ - Λ -interaction following the functional form proposed by Balberg and Gal [27] (see eq. (9)) and obeying the condition $U_{\Lambda}^{(\Lambda)}(n_0/5) = -0.67 \text{ MeV}$, with $\gamma=2$ and $a_{\Lambda\Lambda} = -1200, -200 \text{ MeV fm}^3$ and, respectively, $\gamma=2$ and $a_{\Lambda\Lambda}=0$ and $c_{\Lambda\Lambda}=30000 \text{ MeV fm}^{3\gamma}$. (c) Gravitational mass as solution of the TOV equations as a function of central baryon number density for the cases considered at (b).

spond, respectively, to phase coexistence ($a_{\Lambda\Lambda} = -1200 \text{ MeV fm}^3$) and stability with respect to phase separation ($a_{\Lambda\Lambda} = -200 \text{ MeV fm}^3$) in symmetric (N, Λ) -matter. For the sake of the argument, the case of a purely repulsive and very strong $\Lambda\Lambda$ interaction characterized by ($\gamma = 2, a_{\Lambda\Lambda} = 0, c_{\Lambda\Lambda} = 3 \cdot 10^4$) is considered, too. We can see that employing a strongly attractive coupling at low densities does only slightly shift the density threshold for Λ -production with respect to a weakly attractive coupling, but strongly enhances the equilibrium abundances just above threshold. As we have already noted several times, a strong attraction at low density is correlated to a strong repulsion at high densities, leading to a relative decrease of the Λ abundances at higher densities with smaller values of $a_{\Lambda\Lambda}$. As a consequence, too, decreasing $a_{\Lambda\Lambda}$ leads to an increase of the maximum NS mass. Though, the $2 M_{\odot}$ neutron star limit is not reached. In conclusion, we can say that the ad-hoc inclusion of an extra term in the BSL functional effectively accounting for the missing Y - Y interaction does not solve the well-known neutron star maximum mass problem of the BHF theory.

VII. CONCLUSIONS

In this work, we have presented a complete study of the low temperature phase diagram of baryonic matter including hyperonic degrees of freedom within the phenomenological non-relativistic Balberg and Gal model [27]. We have shown that the hyperon production thresholds are systematically associated with thermodynamic instabilities, leading to distinct first order phase transitions. These transitions can merge into a wide coexistence zone if the production thresholds of different hyperonic species are sufficiently close. As a consequence, a huge part of the phase diagram corresponds to phase coexistence between low-strangeness and high-strangeness phases.

In contrast to the nuclear liquid-gas phase transition which is strongly quenched, this result is only slightly affected by adding electrons and positrons to fulfill the charge neutrality constraint. The only effect is a rotation of the direction of phase separation which reduces the electric charge density component of the order parameter. The reason is that this phase transition is driven mainly by the strangeness degree of freedom, such that the electric charge plays only a minor role. In the latter respect, we thus confirm the finding for the (n, p, Λ, e) -system of Ref. [16] even in the presence of charged hyperons.

Along the beta-equilibrium trajectory with $\mu_L = 0$ the phase coexistence region corresponding to the pop up of Λ - and Σ -hyperons, as predicted by the parameterization BGI, extends over $0.3 \leq n_B \leq 0.4 \text{ fm}^{-3}$. Physically this path is explored by neutron stars with untrapped neutrinos. Following the study in the simple (n, p, Λ, e) -model in Ref. [16], we expect that this phase coexistence region remains at higher temperatures and extends over density and lepton fraction $Y_L = n_L/n_B$ domains explored by warm proto-neutron star matter. A more quantitative analysis is left for future work.

The possible existence of such a phase transition is strongly conditioned by the N - Y and Y - Y interaction. In the second part

of the paper we have thus investigated on the one hand the dependence of the phase diagram on the interaction parameters within the phenomenological BG energy density functional and on the other hand, we have compared the results with an energy density functional based on microscopic BHF calculations by Burgio, Schulze and Li [20]. A complete parameter study of the energy functional would be very cumbersome and not very illuminating, because of the huge number of insufficiently constrained couplings. We have therefore considered the simplified situation of nuclear matter with Λ -hyperons. The phase diagram of this simple model is very similar to the one obtained including the full baryonic octet at densities below the threshold of appearance of more massive hyperons. We therefore believe that this simple model can give correct qualitative results for the full problem.

Both, N - Y and Y - Y -couplings are seen to play a role in determining the existence of an instability. Within the BG model it is shown that an instability exists over a very large parameter domain and the two solar mass limit of NS is compatible with important hyperonic abundances. At variance, BSL is stable with respect to phase separation. Though, phase instability can be reached when the original interaction potential is supplemented with a phenomenological Y - Y interaction. We have considered both pure repulsive and attractive-repulsive

potentials who fit the experimental data, the measurement of a positive bond energy in double- Λ hypernuclei. The results show that an extra Y - Y interaction always results in an enhanced maximum NS mass.

In conclusion, we believe that there is no hyperon puzzle in the sense that the $2M_{\odot}$ neutron star mass value is well compatible with important hyperonic content and, at the same time, the available constraints on the hyperon couplings.

Though, whether hyperons in neutron stars experience a phase transition is a question which requires more constraints from the experimental side.

Acknowledgments

This work has been partially funded by the SN2NS project ANR-10-BLAN-0503 and it has been supported by New-Compstar, COST Action MP1304. Ad. R. R acknowledges partial support from the Romanian National Authority for Scientific Research under grants PN-II-ID-PCE-2011-3-0092 and PN 09 37 01 05 and kind hospitality from LPC-Caen and LUTH-Meudon.

-
- [1] N. Glendenning, Phys. Lett. **B114**, 392 (1982).
 - [2] P. Demorest *et al.*, Nature **467** 1081 (2010).
 - [3] J. Antoniadis, P.C.C. Freire, N. Wex *et al.*, Science, 340, 6131 (2013).
 - [4] M. Oertel, A. F. Fantina, and J. Novak Phys. Rev. C **85**, 055806 (2012).
 - [5] L. Bonanno and A. Sedrakian, Astron. Astrophys. **529**, A16 (2012).
 - [6] S. Weissenborn, D. Chatterjee and J. Schaffner-Bielich, Nucl. Phys. **A881**, 62 (2012).
 - [7] I. Bednarek, P. Haensel, J.L. Zdunik, M. Bejger, and R. Manka, Astron. Astrophys. **543**, A157 (2012).
 - [8] S. Weissenborn, D. Chatterjee and J. Schaffner-Bielich, Phys. Rev. C **85**, 065802 (2012).
 - [9] J. L. Zdunik and P. Haensel, Astron. Astrophys. **551** (2013) A61.
 - [10] P. Haensel and O.Yu. Gnedin, Astron. Astrophys. **290**, 458 (1994).
 - [11] C. Schaab, F. Weber, M.K. Weigel, N.K. Glendenning, Nucl. Phys. **A605** (1996) 531.
 - [12] C. Schaab, S. Balberg, J. Schaffner-Bielich, Astrophys. J. 504, L99 (1998).
 - [13] D. Chatterjee, D. Bandyopadhyay, Phys. Rev. D **74**, 023003 (2006); D. Chatterjee, D. Bandyopadhyay, Astrophys. J. 680, 686 (2008); M. Sinha, D. Bandyopadhyay, Phys. Rev. D **79**, 123001 (2009); T.K. Jha, H. Mishra, V. Sreekanth, Phys. Rev. C **82**, 025803 (2010).
 - [14] J. Schaffner-Bielich, M. Hanauske, H. Stocker and W. Greiner, Phys. Rev. Lett. **89** (2002) 171101.
 - [15] F. Gulminelli, Ad. R. Raduta, and M. Oertel Phys. Rev. C **86**, 025805 (2012).
 - [16] F. Gulminelli, Ad. R. Raduta, M. Oertel, and J. Margueron, Phys. Rev. C **87**, 055809 (2013).
 - [17] B. Peres, M. Oertel, J. Novak, Phys. Rev. D **87**, 043006 (2013).
 - [18] S. Aoki *et al.*, Nucl. Phys. **A828**, 191 (2009).
 - [19] J. K. Ahn *et al.*, Phys. Rev. C **88**, 014003 (2013).
 - [20] G. F. Burgio, H.-J. Schulze, and A. Li, Phys. Rev. C **83**, 025804 (2011).
 - [21] P. H. Pile *et al.*, Phys. Rev. Lett. **66**, 2585 (1991); T. Hasegawa *et al.*, Phys. Rev. C **53**, 1210 (1996); H. Hotchi *et al.*, Phys. Rev. C **64**, 044302 (2001).
 - [22] P. Khaustov *et al.*, Phys. Rev. C **61**, 054603 (2000).
 - [23] P. K. Saha *et al.*, Phys. Rev. C **70**, 044613 (2004); M. Kohno, Y. Fujiwara, Y. Watanabe, K. Ogata, and M. Kawai, Phys. Rev. C **74**, 064613 (2006).
 - [24] T. Nagae *et al.*, Phys. Rev. Lett. **80**, 1605 (1998).
 - [25] G. B. Franklin, Nucl. Phys. **A585**, 83c (1995).
 - [26] I. Vidana, A. Polls, A. Ramos, and H.-J. Schulze, Phys. Rev. C **64**, 044301 (2001).
 - [27] S. Balberg, and A. Gal, Nucl. Phys. **A625**, 435 (1997).
 - [28] M. Oertel, C. Providencia *et al.*, in preparation.
 - [29] C. Ducoin, Ph. Chomaz, and F. Gulminelli, Nucl. Phys. **A771**, 68 (2006).
 - [30] J. M. Lattimer and F. D. Swesty, Nucl. Phys. **A535**, 331 (1991).
 - [31] C. Ducoin, Ph. Chomaz, F. Gulminelli, Nucl. Phys. **A789**, 403 (2007).
 - [32] C. Providencia, L. Brito, S. S. Avancini, D. P. Menezes and Ph. Chomaz, Phys. Rev. C **73**, 025805 (2006).
 - [33] R. C. Tolman, Proc. Nat. Sci. USA 20,3 (1934); J. R. Oppenheimer and G. M. Volkoff, Phys. Rev. 55, 374 (1939).
 - [34] J. Cugnon, A. Lejeune, and H.-J. Schulze, Phys. Rev. C **62**, 064308 (2000).
 - [35] X.-R. Zhou, H.-J. Schulze, H. Sagawa, C.-X. Wu, and E.-G. Zhao, Phys. Rev. C **76**, 034312 (2007), ISSN 0556-2813.
 - [36] H.-J. Schulze, Nucl. Phys. **A835**, 19 (2010), ISSN 03759474.
 - [37] H.-J. Schulze and T. Rijken, Phys. Rev. C **84**, 035801 (2011).

[38] This temperature value has been chosen for computational convenience. The presented results are very close to the zero tem-

perature limit.